

Combinatorial Complexity of 5' Alternative Acetylcholinesterase Transcripts and Protein Products*[§]

Received for publication, March 11, 2004, and in revised form, April 26, 2004
Published, JBC Papers in Press, April 28, 2004, DOI 10.1074/jbc.M402752200

Eran Meshorer^{‡§}, Debra Toiber[‡], Dror Zurel[‡], Iman Sahly^{¶¶}, Amir Dori[‡], Emanuela Cagnano^{**},
Letizia Schreiber^{‡‡}, Dan Grisaru^{§§}, François Tronche[¶], and Hermona Soreq^{‡¶¶}

From the [‡]Department of Biological Chemistry and the Israel Center of Neuronal Computation, Institute of Life Sciences, The Hebrew University of Jerusalem, Jerusalem 91904, Israel, [¶]CNRS FRE2401, Molecular Genetics, Neurophysiology, and Behavior, Institute of Biology, Collège de France, 11 place Marcelin Berthelot, 75231 Paris Cedex 5, France, the ^{**}Department of Pathology, Soroka University Medical Center, Beer-Sheva 64239, Israel, and the Departments of ^{‡‡}Pathology and ^{§§}Obstetrics and Gynecology, Sourasky Medical Center, Tel-Aviv University, Tel-Aviv 84105, Israel

To explore the scope and significance of alternate promoter usage and its putative inter-relationship to alternative splicing, we searched expression sequence tags for the 5' region of acetylcholinesterase (ACHE) genes. Three and five novel first exons were identified in human and mouse ACHE genes, respectively. Reverse transcription-PCR and *in situ* hybridization validated most of the predicted transcripts, and sequence analyses of the corresponding genomic DNA regions suggest evolutionarily conserved promoters for each of the novel exons identified. Distinct tissue specificity and stress-related expression patterns of these exons predict combinatorial complexity with known 3' alternative AChE mRNA transcripts. Unexpectedly one of the 5' exons encodes an extended N terminus in-frame with the known AChE sequence, extending the increased complexity to the protein level. The resultant membrane variant(s), designated N-AChE, is developmentally regulated in human brain neurons and blood mononuclear cells. Alternative promoter usage combined with alternative splicing may thus lead to stress-dependent combinatorial complexity of AChE mRNA transcripts and their protein products.

Alternative splicing and alternate promoter usage both expand the complexity of gene products. While the massive contribution of alternative splicing to such expansion is widely recognized (1), less is known about the scope and significance of alternate promoter usage. Moreover the directionality of transcription processes raises the yet unresolved possibility that

these two phenomena are inter-related, namely that the choice of the first exon determines downstream splice choices (2). The recent accumulation of genomic and gene expression data bases together with the development of sophisticated bioinformatic tools makes these questions amenable for experimental analysis as multiple gene products display both alternate promoter usage and alternative splicing variations. By alignment of expression sequence tags (ESTs)¹ against genomic sequences, for example, it is possible to explore the different alternatively spliced products of a single gene (3, 4). However, EST data bases are biased toward the 3' end of mRNAs and occasionally contain genomic contaminations that may cause misinterpretation of the genomic information (5). To correctly evaluate the inter-relationship between alternate promoter usage and alternative splicing, it is therefore necessary to characterize the identified variants using traditional molecular biology tools at the RNA level and, if applicable, at the protein level as well.

The acetylcholine-hydrolyzing enzyme acetylcholinesterase (AChE) provides an adequate example for such a study. AChE pre-mRNA is subject to stimulus-induced 3' alternative splicing (6), and previous evidence has suggested that it is also subject to alternate promoter usage (7, 8). We analyzed the genomic regions flanking the human and mouse ACHE genes and found an unexpected, evolutionarily conserved diversity of alternate exons at their 5' end. The newly identified exons are stress- and glucocorticoid-regulated and show no apparent connection to the 3' splice variations. One of these new exons was further found to initiate an N-terminal extension to the canonic AChE protein, enabling a combinatorial complexity of developmentally controlled human membrane AChE protein variant(s). Our findings highlight independent yet inter-related expansions of ACHE gene products by 5' and 3' variations in AChE mRNA.

EXPERIMENTAL PROCEDURES

Human Tissues—The use of human embryos, cord blood, and adult tissues in this study was approved by the Tel-Aviv Sourasky Medical

* This research was supported by Israel Science Fund Grant 618y02, United States Army Medical Research and Materiel Command Grant DAMD 17-99-1-9547, European Union Grant QLK3-CT-2002-02062, and Ester Neuroscience, Tel-Aviv (to H. S.) as well as by the Leo Meintz Fund, Tel-Aviv University (to D. G.). Research in Paris was supported by the "Fondation de la Recherche Médicale" and "ACI Integrative Biology." The costs of publication of this article were defrayed in part by the payment of page charges. This article must therefore be hereby marked "advertisement" in accordance with 18 U.S.C. Section 1734 solely to indicate this fact.

The nucleotide sequence(s) reported in this paper has been submitted to the GenBank™/EBI Data Bank with accession number(s) AY389982, AY389981, AY389980, and AY389977.

[§] The on-line version of this article (available at <http://www.jbc.org>) contains Supplemental Tables 1 and 2.

[¶] An incumbent of the Hebrew University's Rector Fellowship and a Golda Meir fellow. Present address: NCI, National Institutes of Health, 41 Library Dr., Bethesda, MD 20892.

^{¶¶} A fellow of the Del Duca Foundation and CNRS.

^{¶¶¶} To whom correspondence should be addressed. Fax: 972-2-6520258; E-mail: soreq@cc.huji.ac.il.

TABLE I
Alternative 5' exons of mouse acetylcholinesterase

Exon	Number of ESTs	Representative EST evidence	Position ^a (from ATG)	Intron size	Splice sites	ORF	Previous reference	Confirmation
				<i>nt</i>				
ME1a	1	BB606349, eyeball, P0	787 to 680	657	GT-AG	No		Yes
ME1b	0		945 to 733	710	GT-AG	No		Yes
ME1c-long	1	AK036443, bone, adult	1762 to 22			No		No
ME1c	18	BB639234, thymus, P3	1762 to 1671	1648	GT-AG	No	10	Yes
ME1d	0		2271 to 1980	1957	GT-AG	No	8	Yes
ME1d'	0		2271 to 2008	1986	GT-AG	No		Yes
ME1e	0		2518 to 2403	2380	GT-AG	Yes		No

^a For convenience, the – in front of all position numbers was eliminated.

Center Ethics Committee according to the regulations of the Helsinki accords. Tissue samples from spontaneously aborted human fetuses at different ages (16, 25, and 34 gestational weeks) were transferred immediately to 4% paraformaldehyde, embedded in paraffin, and sliced (7 μ m). Fresh samples of umbilical cord blood cells were obtained following normal deliveries. Adult human brain samples were collected within 4 h postmortem from a 70-year-old patient with cardiac arrhythmia. Tissues were frozen immediately in liquid nitrogen. Brain homogenates (in 0.1 M phosphate buffer, 1% Triton X-100) were immunoblotted using standard procedures.

Animals—Central nervous system-specific glucocorticoid receptor (GR) mutants (GR^{NesCre}), control littermates (GR^{LoxP/LoxP}) (9), and FVB/N male mice were kept under a 12-h dark/12-h light diurnal schedule with food and water *ad libitum*. Stress experiments included a 30-min immobilization in 50-ml conical tubes. Mice were sacrificed by decapitation 2 h after immobilization, and brains were dissected on ice, frozen in liquid nitrogen or fixed in 4% paraformaldehyde for 24 h, embedded in paraffin, sliced to 5–7- μ m sections, and collected by adhesion to Superfrost®-Plus slides (Menzel-Glaser, Braunschweig, Germany). For all experiments, naive age-matched males served as controls. These experiments were approved by the animal committee in the Hebrew University.

Computational Resources—The human (GenBankTM accession number AF002993) and mouse (GenBankTM accession number AF312033) *ACHE* loci were analyzed using the National Center for Biotechnology Information for access to the GenBankTM as well as to Blast, Entrez, Locus Link, Structure, Protein, and OMIM (Online Mendelian Inheritance in Man) data base resources. Expert Protein Analysis System at the Swiss Institute of Bioinformatics was used for access to a variety of data manipulation programs and protein data bases. The Baylor College of Medicine Search Launcher² served for data manipulation and to derive display programs. The MatInspector program at Genomatix or the Cister software³ was used to find transcription factor binding sites.

RNA Extraction and cDNA Preparation—Total RNA was extracted from animal and human tissues using the EZ-RNA total RNA isolation kit (Biological Industries, Beit Haemek, Israel) as instructed, diluted in diethyl pyrocarbonate-treated water to a concentration of 100 ng/ μ l, and stored at –70 °C until use. Human RNA from leukemic T-lymphocytes, liver, and testis was obtained from Ambion (Austin, TX). SuperScript reverse transcriptase (Invitrogen) was used with either poly(dT) or random hexamers. Gene-specific primers (see below) were used for one-step RT-PCR (Qiagen, Hilden, Germany).

Fluorescence in Situ Hybridization (FISH)—Paraffin-embedded sections (mouse horizontal whole brain sections or human sagittal sections from whole embryos or human adult prefrontal cortex) were subjected to deparaffination with xylene (two 5-min washes) followed by decreasing ethanol washes (100, 75, 50, and 25%) and then a wash in phosphate-buffered saline with 0.5% Tween 20 and incubation with 10 mg/ml proteinase K (8 min at room temperature). Hybridization in a humidified chamber involved 10 mg/ml probe (in 50% formamide, 5 \times SSC, 10 mg/ml tRNA, 10 mg/ml heparin for 90 min at 52 °C). Sections were then washed twice at 60 °C with 50% formamide, 5 \times SSC, and 0.5% SDS; twice in 50% formamide, 2 \times SSC at 60 °C; and twice in Tris-buffered saline + 0.1% Tween 20 (TBST) at room temperature and then blocked in 1% skim milk (Bio-Rad) for 30 min.

Biotin-labeled probes (see Supplemental Table I) were detected by incubating sections with streptavidin-Cy3 conjugates (CyDyeTM, Amer sham Biosciences) for 30 min followed by three washes in TBST. Sections were mounted with IMMU-MOUNT (Shandon Inc., Pittsburgh, PA).

Polymerase Chain Reaction—PCR was used for detecting different transcripts in various tissues and to confirm sequences. The PCR mixture contained 2 units of *Taq* DNA polymerase (Sigma), deoxynucleotide mixture (0.2 mM each) (Sigma), forward/reverse primers (see Supplemental Table II, 0.5 μ M each), and 300 ng of template (cDNA or genomic DNA). Each of the 35 cycles included denaturation (1 min at 95 °C), annealing (1 min at 60 °C), and elongation (72 °C at 1 min).

Antibodies—High affinity polyclonal rabbit IgG antibodies against the human hE1d-encoded N-terminal domain were custom-made (Eurogentec, Seraing, Belgium). Two 16-amino acid residue peptides from the coding sequence of human exon hE1d (hN-AChE) were synthesized (KVRSHPSGNQHRPTRG and GRSFHCRRGVRPRPA), mixed, and injected together into two rabbits. Additional boost injections were given at 2, 4, and 8 weeks thereafter. Final bleeding was carried out after week 16. Enzyme-linked immunosorbent assay screening with the synthetic peptides served to identify successful antibody production. The synthetic peptides were further used for affinity purification of the antibodies. Dilutions of 1:500 of the affinity-purified antiserum were used for Western blotting.

Flow Cytometry—Mononuclear fractions of cord blood cells were separated by FACS lysing solution (BD Biosciences, diluted 1:100 in double-distilled water, 12-min incubation). Cells were either stained directly with phycoerythrin-conjugated CD34 (BD Biosciences), allophycocyanine-conjugated CD3 (Caltag, Burlingame, CA), allophycocyanine-conjugated CD19 (BD Biosciences), peridinin chlorophyll protein-conjugated CD45 (BD Biosciences), and phycoerythrin-conjugated interleukin 7 (R&D Systems Inc., Minneapolis, MN) antibodies or first permeabilized and fixed (Fix and Perm kit, Caltag; 7 min) and then stained. Isotype controls served to distinguish unspecific labeling. Rabbit anti-hN-AChE antibodies were detected on these cells using fluorescein isothiocyanate-conjugated goat anti-rabbit Fab antibodies (Jackson ImmunoResearch Laboratories, Inc., Westgrove, PA). Multiparameter flow cytometry was performed using the FACScalibur flow cytometry system (BD Biosciences) equipped with Cellquest software (BD Biosciences). hN-AChE expression was assessed in fresh CD45⁺ cells by analyzing 50,000 gated events.

RESULTS

5' Diversity of Murine AChE mRNAs—EST data base searches using the 5' region of the mouse (m) *ACHE* gene revealed the existence of five putative alternative first exons (Table I and Fig. 1A). The most proximal exon was termed mE1a. The EST clone containing this sequence (GenBankTM accession number BB606349, mouse eyeball) extends from position –787 to –680 (relative to the translational ATG start present in the mouse exon 2) and continues with exon 2 (Fig. 1, A and B), skipping over a 657-nucleotide (nt) intron (termed mouse mI1a) that possesses consensus GT-AG splice sites. RT-PCR and sequencing confirmed the existence of this transcript in the mouse cortex (GenBankTM deposit, accession number AY389982).

A second first exon, named mE1b, was found by RT-PCR using a forward primer located in the –945 to –923 region with a reverse primer on exon 2 (see Supplemental Table II). The resulting product extends from this primer to position –733 and skips over a 710-nt intron (mI1b), which includes consensus GT-AG splice sites (Fig. 1, A and B). This exon as well was confirmed in the mouse cortex by RT-PCR and sequencing (GenBankTM deposit, accession number AY389981).

Upstream to mE1b, at –1762 to –1671, we found the “clas-

² See searchlauncher.bcm.tmc.edu.

³ See zlab.bu.edu/~mfrith/cister.shtml.

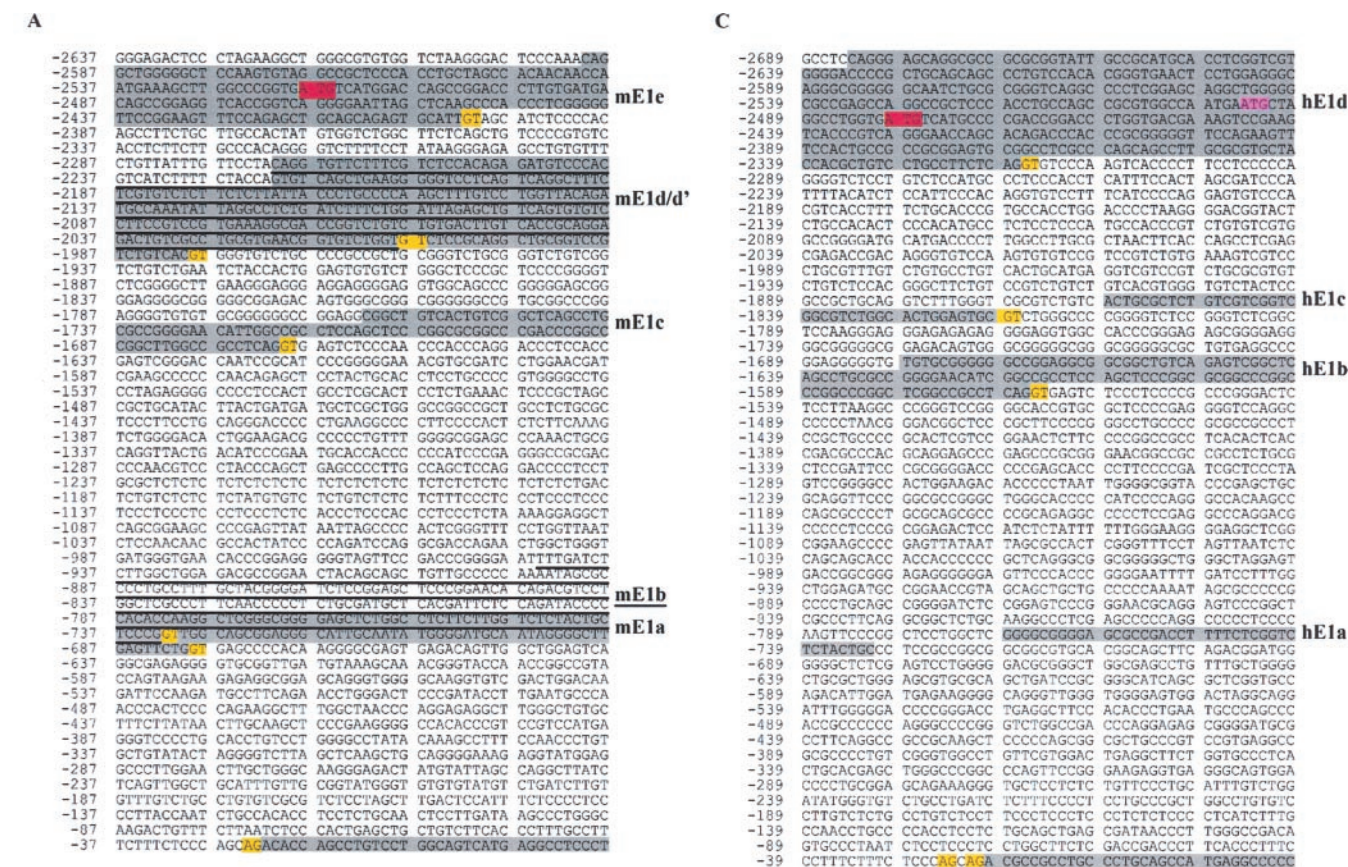


FIG. 1. Mouse and human 5' genomic regions and 5' transcripts. *A*, 2.6 kb of the 5' genomic region of the mouse *ACHE* gene are shown. Exons (shaded gray or underlined) are named on the right. Splice sites are shown in yellow, and translation start sites are shown in red. The bottom line shows the beginning of exon 2. *B*, schematic representation of the entire 5' putative transcribed region of the *ACHE* gene containing the variant exons. All schemes are drawn to scale. Exons verified by sequencing are painted *aquamarine* and are connected by *solid lines* to exon 2 (*mE2*). A non-verified exon, in brackets, is *white* and connected by a *dashed red line*. The long cDNA clone (GenBank™ accession number AK036443, *mE1c-long*) is shown in gray. The ORF of *mE1e* is red, and the one in *E2* is orange. *C* and *D*, 2.65 kb of the 5' region of the human *ACHE* gene and the corresponding scheme are shown. The two possible starting ATGs for *hE1d* are shown in pink and red. The second ATG corresponds to the ATG of *mE1e* (see Fig. 6*B* below).

sical" exon 1 (10), renamed here *mE1c*, in 18 different reported homologous EST clones (GenBank™ accession number BB639234, Table I). When this first exon is fused to exon 2, a 1648-nt intron (*mI1c*) that contains consensus GT-AG splice sites is spliced out. Sequencing of an RT-PCR-amplified DNA fragment confirmed the existence of *mE1c* in the mouse cortex.

An additional mRNA transcript that contains *mE1c* but proceeds through the genomic sequence was named *mE1c-long*. Two longer ESTs indeed initiated at *mE1c* (GenBank™ accession numbers BB629342, adult bone, and CA327701, whole brain embryo) and extend through the entire genomic sequence to exon 2 (GenBank™ accession number AK036443, adult male bone). In these ESTs, exon 2 is fused to exon 3. Splicing of intron 2 rules out the possibility of genomic DNA contamination as the source of this *mE1c-long* variant.

Further upstream, an alternative first exon (8) had previously been found at position -2271 to -1980 followed by a 1957-nt intron (*mI1d*). This first exon was found to be fused

with exon 2. We confirmed the expression of the corresponding transcript in the prefrontal cortex by RT-PCR and sequencing. This exon was named *mE1d*. Two alternative splice donors that differ by 29 nucleotides were observed in the mouse cortex. We named the shorter form *mE1d'* (GenBank™ deposit, accession number AY389980).

Upstream from *mE1d*, three different putative ORFs (positions -2518 to -2402, -2925 to -2522, and -3129 to -2933) were found in a continuous reading frame with that of the classical protein. These could add 46, 142, or 73 amino acids (respectively) to the common ORF beginning at exon 2. Of these, the *mE1e* ORF shares 79% sequence similarity with the corresponding region in the human *ACHE* gene and its translated sequence (see below) and was thus regarded as a candidate. Fig. 1, *A* and *B*, depicts the different mouse 5' exons.

5' Diversity of Human AChE mRNAs—EST data base searches using the 5' region of the human (h) *ACHE* gene revealed the existence of at least four alternative first exons

TABLE II
Alternative 5' exons of human acetylcholinesterase

Exon	Number of ESTs	Representative EST evidence	Position ^a (from ATG)	Intron size	Splice sites	ORF	Exon 2 start	Previous reference	Confirmation
				<i>nt</i>					
hE1a	1	BB606349, eyeball, P0	768 to 732			No			No
hE1b	23	BG707892, hypothalamus	1681 to 1576	1543	GT-AG	No	CAG	11	Yes
hE1c	1	BI667712, hypothalamus	1859 to 1824	1803	GT-AG	No	ACG		No
hE1d	3	BX420294, fetal brain	2720 to 2318	2294	GT-AG	Yes	ACG		Yes

^a For convenience, the – in front of all position numbers was eliminated.

(Table II). The previously identified mouse EST clone (mE1a GenBankTM accession number BB606349, see above) suggests the existence of the alternative first exon named hE1a.

The known first exon at –1681 to –1576 (relative to the translational start site ATG present in the human exon 2) (11) is named here hE1b (represented by EST clone GenBankTM accession number BG707892, human brain hypothalamus). A 1543-nt intron (hI1b) separates hE1b from exon 2 (position –23). We confirmed the existence of hE1b by RT-PCR and sequencing.

An additional EST clone contained the genomic sequence located at position –1859 to –1824 (GenBankTM accession number BI667712, human brain hypothalamus). This putative first exon, fused to exon 2 at position –20 (ACG), was named hE1c. The corresponding 1803-nt intron (hI1c) includes donor and acceptor splice sites (GT-AG). Exon 2 starts with two optional acceptor splice sites located 3 nucleotides apart (both AG dinucleotide; Fig. 1, C and D). Therefore, when fused to hE1c, exon 2 starts at a different position than the one described previously. Our attempts to confirm the existence of this transcript failed.

An additional EST clone (GenBankTM accession number BX420294, human fetal brain) contained a putative first exon located further upstream at position –2720 to –2318 (exon hE1d) fused to exon 2 at position –20. This implies the existence of a 2294-nt intron (hI1d). The existence of this mRNA was confirmed by RT-PCR and sequencing (GenBankTM deposit, accession number AY389977; Fig. 1, C and D). Intriguingly hE1d harbors a translation start codon (ATG, position –2495) creating a continuous reading frame with that of the classical ATG in exon 2 (12), thus potentially adding 66 amino acids to the AChE protein. An additional ATG (position –2478) in the same ORF may yield a shorter 61-amino acid domain. Sequence homology with mE1e, which lacks the first ATG, suggests that the second ATG is more likely to serve as the translational start site.

Putative Promoters for the Novel Exons—Using luciferase assays, Atanasova *et al.* (8) demonstrated the functionality of the promoter located upstream to mE1d (referred to in their work as exon E1a). In our study, the Cister and Chip2Promoter programs enabled promoter predictions, which are shown in Fig. 2A for the murine and human *ACHE* genes. These programs search for regions with motif conservation predicting high probability of being transcriptionally active promoters. These are based primarily on the density of putative transcription factor binding sites. Several regions with such high probability were revealed by this search. Promoter prediction analyses of the region containing the novel alternative first exons revealed a plausible promoter for each of the newly identified exons of both the mouse and human genes (Fig. 2, A and B). The probability score of the alternative promoters was found to be similar to that of the previously described promoter (upstream to mE1b in mouse and hE1b in human), supporting the notion that they might be functionally active. A particularly high probability to function as a promoter was observed for the mouse region upstream to exon mE1a. In the human gene, we identified hE1a based on homology to the mouse mE1a. Exon

hE1a is a weak candidate for being a true exon because it lacks consensus splice sites and because no ESTs were found in the entire region between exon 2 and exon hE1b in the human sequence. Intriguingly the region located upstream from hE1a displays the highest probability of functioning as a promoter (Fig. 2A), perhaps suggesting a change in function for this sequence during evolution. The Cister and the Chip2Promoter program, which does not apply to murine sequences, yielded similar predictions for human promoters.

A closer look at the distribution of the transcription factor binding sites revealed that most sites are common to several of the putative alternative promoters and evolutionarily conserved in both human and mouse. Several putative DNA targets, however, were unique to one of the identified promoters. For example, a conserved binding site for the transcription factor Dlx, highly expressed during organ development (13), was found in mP1 and hP1, and a putative binding site for transforming growth intestinal factor was found in mP2 and hP2. Of interest, three putative glucocorticoid response elements (GREs) were identified in the upstream region of the human *ACHE* gene (one in hP3 and one adjacent to hE1a, Fig. 2A), and one was identified in the mouse gene (mP2, Fig. 2A). It was therefore tempting to test the glucocorticoid and/or stress response of these newly identified transcripts.

Short Interspersed Nuclear Elements (SINEs) and Long Interspersed Nuclear Elements (LINEs) Separate 5' Alternative Exons from the Distal Human *ACHE* Promoter—On average, one might expect one SINE and one LINE for approximately every 2–3.5 kb except within the transcription unit itself (14). A totally different outcome emerged for the currently available GenBankTM *ACHE* sequences (20 kb of the human, GenBankTM accession number AF002993, and 9.5 kb of mouse, GenBankTM accession number AF312033) upstream to the translation start sites of exon 2. The SINE and LINE distributions were analyzed using the Eldorado software (Genomatix) and the RepeatMasker algorithm (Baylor College of Medicine Search Launcher). The density was found to be 6-fold higher than the expected average for SINEs and almost 2-fold higher than the expected average for LINEs (Fig. 2, C and D). This leaves little room for any functional DNA in this area. In contrast, exceptionally few repeats (one and three, respectively) were found within the human and mouse 3.5-kb regions where the alternative first exons were identified, supporting a functional role for these DNA fragments in human and mouse. The closest gene upstream to *ACHE* is located ~180 kb away (15).

Tissue Distribution of the Novel Exons in Mouse—Tissue distribution in mouse of the mRNAs containing the different alternative first exons was studied by RT-PCR (Fig. 3A). Exon mE1a was found to be expressed in every examined brain region, including hippocampus, cortex, PFC, brainstem, and basal nuclei. Exon mE1a was also expressed in the thymus, heart, liver, intestine, and spleen but not in kidney, testis, muscle, or spinal cord. Exon mE1b was detected in most of the tissues examined with the exception of liver, intestine, and muscle. Exon mE1c was the most widely expressed. It was, however, absent from intestine. Exon mE1d was detected in the

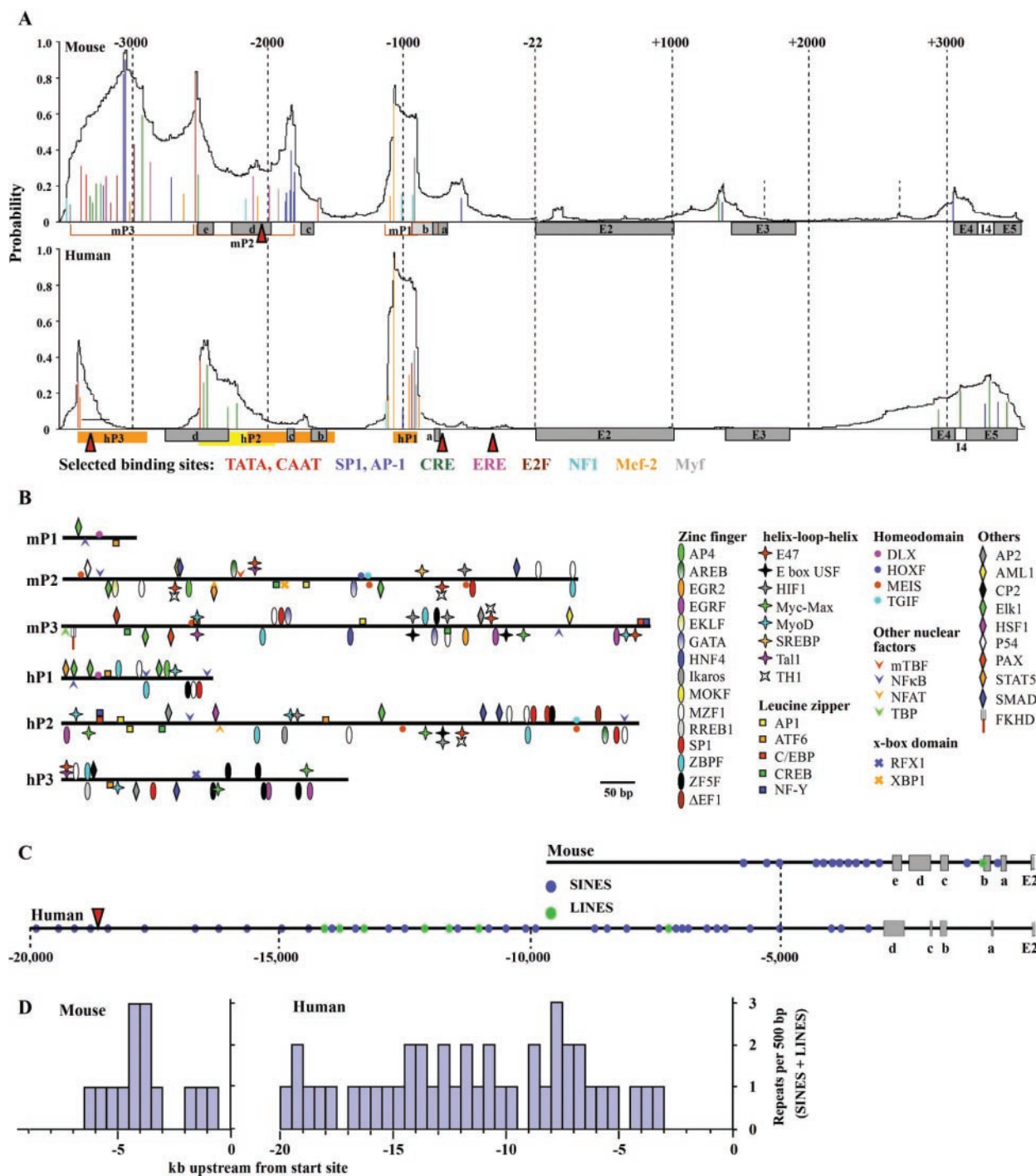


FIG. 2. Promoter and synteny analyses of mouse and human *AChE* genes. *A*, Cister software analysis for 7.1 kb of mouse (*top*) and human (*bottom*) *AChE* genes, including 3.55 kb of upstream sequence and 3.55 kb of the coding region, representing the overall probability for a specific region to function as a promoter. *Colored lines* represent selected transcription factor binding sites detailed below. *Red triangles* represent putative GREs. The different alternative 5' exons (*gray boxes*) are marked *a–e* for mouse and *a–d* for human. Base counts from the starting ATG (+1) are marked *above* (*dashed lines*). For comparison, the human sequence was analyzed with the Chip2Promoter software (Genomatix suite). Human promoter predictions are shown as *orange boxes* (hP1, hP2, and hP3); the gene-associated promoter (hP2, defined by the program as the proximal promoter to the first exon) is shown as a *yellow box*. Chip2Promoter does not support the mouse sequence; therefore the corresponding promoter regions were determined according to Cister and are shown as *empty brick-colored boxes* (mP1, mP2, and mP3; *top*). *B*, MatInspector analysis of the predicted binding sites for transcription factors. Factors have been grouped according to structure, function, motif recognition, or others and are depicted by different *colors and shapes* shown on the *left*. *C* and *D*, SINE (*blue circles*) and LINE (*green circles*) distribution in the upstream regions of mouse (9.5 kb, *top*) and human (20 kb, *bottom*) genes. The distal *AChE* promoter (18) is shown in *red*. Repeat counts for 500 bp are shown in *E* for both mouse (*left*) and human (*right*). *CRE*, cAMP-response element; *ERE*, estrogen response element; *CREB*, cAMP-response element-binding protein; *C/EBP*, CCAAT/enhancer-binding protein; *SREBP*, sterol-regulatory element-binding protein; *TGIF*, transforming growth factor- β -induced factor; *NFAT*, nuclear factor of activated T-cells; *STAT*, signal transducers and activators of transcription; *TBP*, TATA-binding protein; *USF*, upstream stimulatory factor; *HIF1*, hypoxia-inducible factor 1.

brain (hippocampus, PFC, brainstem, and basal nuclei) and heart but not spleen, thymus, intestine, or liver. While it is difficult to compare the expression levels between different

RT-PCR products due to differences in primer and target efficiency, a tissue distribution analysis, as was conducted, gives a good hint of the relative expression levels of each variant in

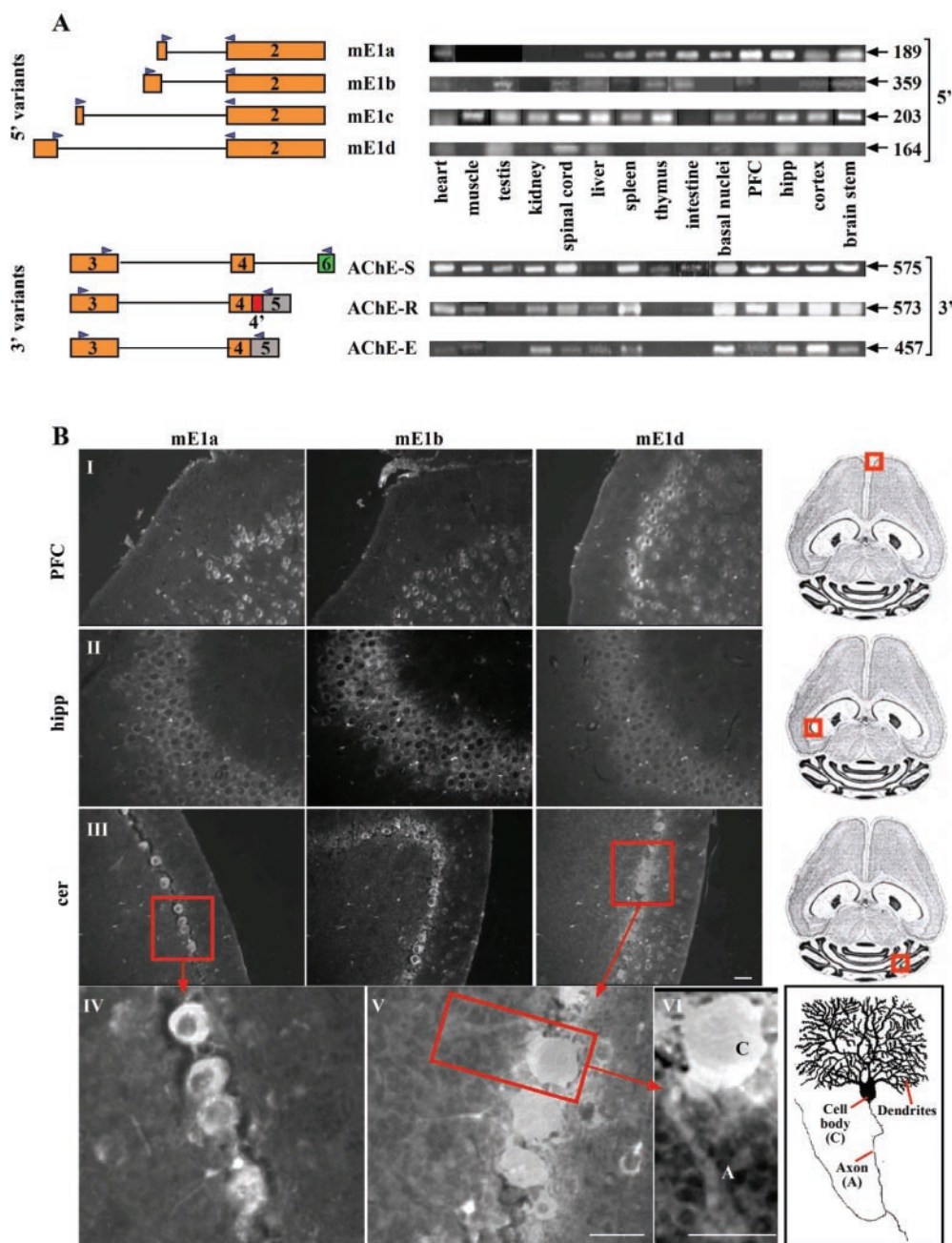


FIG. 3. Tissue and cell type expression patterns of the alternatively spliced transcripts of AChE. *A*, RT-PCR products and their corresponding molecular sizes (*right*) of the 5' (*four upper lanes*, mE1a, mE1b, mE1c, and mE1d) and 3' (*three lower lanes*, AChE-S, AChE-R, and AChE-E) alternative transcripts of murine AChE. Primer positions for each transcript are depicted on the *left diagram* (*triangles*) (for primer sequences, see "Experimental Procedures"). *hipp*, hippocampus. *B*, representative fluorescent images of transcripts including mE1a, mE1b, and mE1d in PFC (*I*), hippocampus (*II*), and cerebellum (*cer*, *III*) of naive FVB/N mice. Schematics on the *right* show the enlarged areas (*red boxes*). Enlargement of a cerebellar area (*boxed*) shows strong cytoplasmic labeling of mE1a (*IV*) and cytoplasmic and nuclear labeling of mE1d (*V*) in Purkinje cells. An enlargement of a single Purkinje cell with a labeled axon is shown in the *bottom right panel* (*VI*) with a schematic drawing on the *right*. Bars, 50 μ m.

each tissue. We conclude that mE1c is the most abundant transcript due to its almost ubiquitous expression and due to its over-representation by ESTs (Table I).

For comparison, we investigated in the same tissues the expression profiles of the different AChE 3' variants. "Synaptic" AChE-S was strongly expressed in all tissues examined except for thymus, liver, and the small intestine where only weak expression was observed, similar to the expression pattern of mE1c. "Read-through" AChE-R was strongly expressed in all of the brain regions tested and in spleen. It was moderately expressed in heart, muscle, kidney, spinal cord, and liver and very poorly expressed in the testis, thymus, and intestine.

"Erythrocytic" AChE-E was expressed in all of the examined brain regions as well as in heart, kidney, spinal cord, liver, spleen, and muscle. It was absent from testis, thymus, and the small intestine. Thus, none of the 5' variants shared the same expression pattern with a single 3' variant, suggesting that 5' splicing patterns do not always dictate 3' splicing in the mature mRNA. The four different 5' and three different 3' splice options may thus potentially yield 12 distinct transcripts.

Distinct Neuronal Distributions of the 5' Murine Exons—To achieve cellular resolution levels for the expression patterns of the novel exons, we designed 40–50-mer 5'-biotinylated fully 2'-*O*-methylated riboprobes for FISH (see "Experimental Pro-

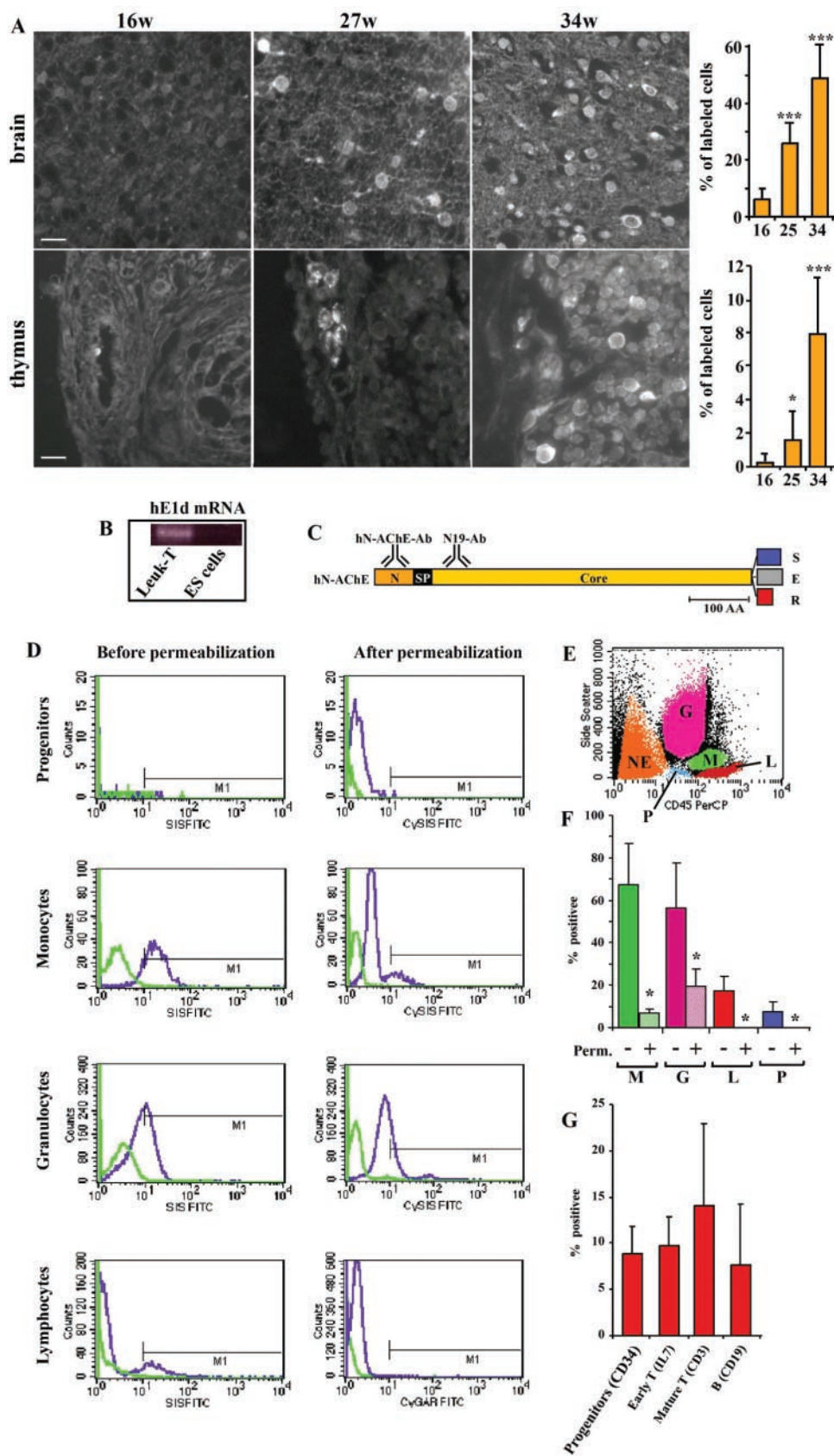


FIG. 4. Human embryonic expression of hN-AChE. **A**, FISH detection of hE1d mRNA in sections from 16- (left), 24- (middle), and 34 (right)-week-old human embryonic brain (top) and thymus (bottom). Bar graphs on the right show fractions of labeled cells (*, $p < 0.05$; ***, $p < 0.0005$; two-tailed Student's t test). **B**, RT-PCR analysis of hE1d mRNA on RNA extracted from human leukemic T-cells (*Leuk-T*, left, Ambion) and human embryonic stem cells (*ES cells*, right). **C**, AChE protein composition and epitope locations of the antibodies used (N, N terminus; SP, signal peptide; Core, AChE core domain). The three different optional C termini are depicted on the right (S, AChE-S; E, AChE-E; R, AChE-R). **D-G**, hematopoietic expression of membranial hN-AChE. **D**, five distinct cell populations were identified by flow cytometry using CD45 detection versus side scatter plot (NE, nucleated erythrocytes; M, monocytes; G, granulocytes; P, progenitors; L, lymphocytes). **E**, hN-AChE labeling (purple) in

cedures" for details). Fig. 3B presents representative FISH profiles for mE1a, mE1b, and mE1d.

These three exons all appeared to be expressed in neurons. They displayed, however, distinct cell type specificities and subcellular distributions. For example, essentially all of the deep layer neurons in the PFC displayed pronounced mE1a levels and considerably lower mE1b labeling. Exon mE1d mRNA was particularly concentrated in the uppermost layer of PFC neurons (Fig. 3B, I), suggesting distinct levels for AChE mRNA transcripts in specific subsets of PFC neurons. Whereas these differences potentially reflect probe efficiencies, they also highlight distinct expression patterns for the various alternative AChE mRNAs. Thus, hippocampal CA2 neurons within the same or adjacent sections displayed consistently low levels of all three exons (Fig. 3B, II), whereas cerebellar neurons showed differential expression of the various 5' exons (Fig. 3B, III). Exon mE1a accumulated in the cytoplasm of Purkinje cell perikarya but was only faintly detected in other cerebellar neurons. mE1b was poorly expressed in the cerebellum, and mE1d was strongly expressed in Purkinje cells in which it was labeled in both cell bodies and axonal processes (Fig. 3B, IV and V). In addition, mE1d was transcribed in other neurons of the cerebellum, including the cells interspersed in the molecular layer. In these neurons, it displayed an asymmetric labeling pattern accompanied by neurite labeling. Granular neurons were poorly labeled with the probe for mE1d.

Human hE1d AChE mRNA Expression—The tissue distribution of transcribed hE1d mRNA in several developmental stages was explored in paraffin sections from human embryos aged 16, 25, and 34 weeks. At week 16, hE1d mRNA was only weakly detected in the nervous system and was absent in the thymus. As development proceeded, hE1d expression became more pronounced with increased density of positive cells and increased labeling intensity in both the nervous system and the thymus. At week 34, up to $50 \pm 10\%$ of the neurons were positive (Fig. 4A). In contrast, as low as $2 \pm 1.5\%$ of the thymus cells were hE1d mRNA-positive at week 25, but by week 34, over $8 \pm 1.5\%$ of the cells were positive ($p < 0.0005$, two-tailed Student's *t* test). Since hE1d demonstrated a developmentally regulated expression pattern, we performed RT-PCR analysis on RNA extracted from human embryonic stem cells (16) and leukemic T-cell lymphocytes. Whereas human embryonic stem cells were RT-PCR negative for hE1d, leukemic T-cells were positive (Fig. 4B).

The developmentally regulated expression of hE1d mRNA in the fetal thymus and in T-cells called for corresponding analysis of its putative translation product, hN-AChE. Rabbit polyclonal antibodies were generated against two short internal peptides from the hN-AChE ORF (Fig. 4B). Although unsatisfactory for immunohistochemistry on paraffin-embedded sections, these anti-hN-AChE antibodies successfully labeled human mononuclear cells in flow cytometry analysis. Cord blood cell lineages were classified according to their relative side scatter and their expression levels of the blood cell marker CD45 into lymphocytes (Fig. 4E, L), monocytes (M), granulocytes (G), blood cell progenitors (P), and nucleated erythrocytes (NE). Monocytes and granulocytes, both of which express AChE (40), displayed the most prominent hN-AChE labeling with 67 ± 19 and $57 \pm 21\%$ of the cells expressing hN-AChE as compared with isotype control. In addition, $17 \pm 7\%$ of the

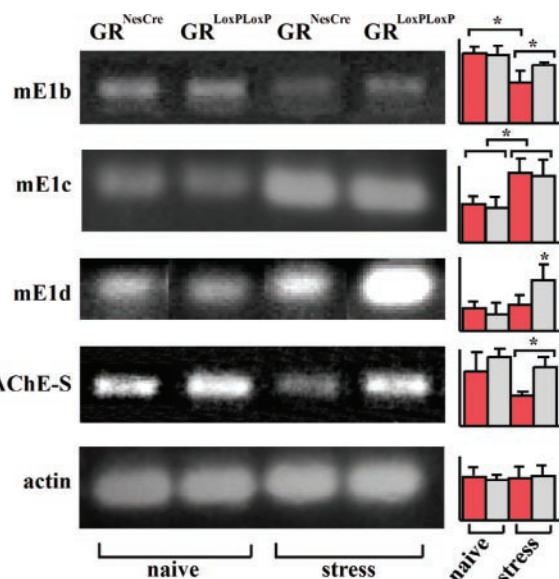


FIG. 5. Stress- and glucocorticoid-related regulation of murine 5' alternative exons. RT-PCR analysis of mE1b, mE1c, mE1d, mAChE-S, and actin in the cortices of neuron-specific GR knock-out (GR^{NesCre}) and control littermate ($GR^{LoxP/LoxP}$) mice 2 h following 30 min of immobilization stress. Actin mRNA served as control. Quantification (against actin levels) is shown on the right (average of three animals in each group). Stars note statistically significant differences from the noted controls ($p < 0.05$, Kruskal-Wallis test).

lymphocytes and $7.5 \pm 4\%$ of the progenitors were hN-AChE-positive (Fig. 4, D and E), while nucleated erythrocytes were negative. To further subclassify the lymphocytes expressing hN-AChE, we used specific markers for undifferentiated cells (CD34), early T-cells (interleukin 7), mature T-cells (CD3), and mature B-cells (CD19). Some of these markers may appear in more than one cell lineage; however, hN-AChE labeling appeared in 9 ± 3 and $10 \pm 3\%$ of the $CD34^+$ undifferentiated cells and early T-cells and increased to $14 \pm 9\%$ in mature T-cells. B-cells presented highly variable ($7.5 \pm 6.5\%$) hN-AChE labeling.

To test whether hN-AChE is membranar, as predicted from its primary structure analysis, the flow cytometry tests were repeated following permeabilization of the cells. Following permeabilization, monocyte and granulocyte labeling decreased to 7 ± 1 and $20 \pm 7.5\%$, respectively, implying that hN-AChE is mainly present at the membrane.

Stress- and Glucocorticoid-associated Expression of the Novel Exons—Stress induces rapid (17) yet long lasting (6) expression of AChE-R mRNA encoding an AChE variant with a cysteine-free C terminus, which leads to the accumulation of stress-associated AChE monomers. The *ACHE* gene possesses a GRE in a distal enhancer (18), and *ACHE* gene expression increases following administration of the murine stress hormone corticosterone (6). We therefore investigated whether any of the novel 5' exons are selectively overproduced following stress in control mice as compared with mutant mice that selectively lack the GR gene in their central nervous system (GR^{NesCre} mice (9)).

In the mouse PFC, mE1b mRNA levels were largely unaltered in the GR^{NesCre} animals as compared with $GR^{LoxP/LoxP}$

monocytes, granulocytes, lymphocytes, and blood cell progenitors. An isotype control (green) was used for comparison. No increase was observed following permeabilization of the cells (right), indicating membranar expression. F, percentage of positive cells before (–) and after permeabilization (+) of the noted $CD45^+$ cell lineages. The average of four different cord blood preparations is shown. G, lymphocyte subclassification. Specific markers (CD34, undifferentiated; interleukin 7 (IL7), early lymphocytes; CD3, mature T-lymphocytes; CD19, mature B-lymphocytes) demonstrate elevated hN-AChE expression in mature T-lymphocytes. FITC, fluorescein isothiocyanate; PerCP, peridinin chlorophyll protein; Perm., permeabilized.

N-AChE Protein Products—Novel 5' extended putative ORFs, in-frame with the known AChE coding sequences, were identified in orthologous regions of the mouse mE1e and the human hE1d exons. The putative ORF of mE1e encodes an additional 46 amino acids with no homology to any known protein in the data base (Fig. 6A). These include 8 positively charged residues (4 arginines, 1 lysine, and 3 histidines) but only 2 negatively charged ones (2 glutamates), yielding an extremely high pI value of 11.54. Secondary structure analysis of the mE1e translation product (mN-AChE) (GOR4 software)⁴ revealed a potential α helical folding (Fig. 6B, top). Motif Scan software analysis⁵ revealed in this peptide a putative protein kinase phosphorylation site (position 4–6, TsR) and an *N*-myristoylation site (position 13–18, GGhrSG, Fig. 6B). An addition of this peptide chain to the N terminus will most likely prevent cleavage of the mouse AChE signal peptide (MRPPWYPLHTPSLAFPLLFLLLSLLGGGARA, position 1–31). This will yield a 77 (46 + 31)-amino acid residue extension of the mN-AChE protein (13.4% increase over the 574 residues of mAChE-S (19)) with the signal peptide predicted to become transmembranal (e.g. the asialoglycoprotein receptor variant (20)).

The corresponding human exon hE1d encodes an N-terminal extension of 66 amino acids in-frame with the hAChE protein (Fig. 6B). This peptide as well precedes the signal peptide (MRPPQCLLHTPSLASPLLLLLLWLLGGGVGA, position 1–31) that is normally cleaved off during maturation. We predicted its presence to prevent AChE cleavage, resulting in a larger protein (by 92 (61 + 31) or 97 (66 + 31) amino acids, 16–17% increase over the 574 residues of AChE-S (12)).

No significant homology was found for the hN-AChE peptide sequence in the Swiss-Prot data base. Similar to mN-AChE, the human peptide includes a putative phosphorylation site (for casein kinase II, position 7–10, ScpD) as well as an *N*-myristoylation site (position 31–36, GGsrSF, Fig. 6A). In addition, similar to mN-AChE, hN-AChE displays an extremely high predicted pI (11.76), matching that of histones and other nucleic acid-binding proteins.⁶

In immunoblots of glioblastoma protein extracts, the polyclonal anti-hN-AChE antibodies labeled an ~66–70-kDa double band comparable to the labeling pattern observed using the commercially available N19 anti-AChE antibody (Fig. 6C, inset, top left). Protein extracts from different regions of the human brain (shown schematically in Fig. 6E) demonstrated a similar size for the hN-AChE protein *in vivo* (Fig. 6C, bottom). Expression spanned various cortical domains, including PFC and the occipital cortex where it was most prominent. The hippocampus, striatum, and amygdala were also positive, but cerebellar expression was very low. To achieve better resolution, we turned to mRNA *in situ* hybridization. FISH analysis of paraffin-embedded human PFC sections revealed prominent neuronal hE1d mRNA labeling with 57 ± 34% of the cells in the PFC being positive. Up to 25% of the labeled cells displayed hE1d mRNA labeling in neuritic processes, reaching 14.5 ± 7.5 μ m in length (Fig. 6D). A significant fraction of the stress-responding PFC neurons thus express hN-AChE both in their cell body and in neurites.

DISCUSSION

The recent availability of human and mouse genomic sequences together with rich EST data bases and advanced computer programs enabled the identification of novel alternative 5' exons and corresponding promoters in the human and mouse

ACHE genes. Two proximal human (18) and mouse (7, 8) *ACHE* promoters have been described previously. In our current study we demonstrate that human and mouse *ACHE* genes contain at least four alternative first exons each of which at least one encodes an extended N terminus. We named the extended AChE protein(s) hN-AChE and found expression of this protein(s) in the nervous system and blood cells during various stages of their development.

Alternative Splicing and Alternative Promoter Usage in AChE—Alternative splicing enables the creation of different mRNAs and different proteins from a single gene, thus increasing the diversity of gene expression and the proteome (1). AChE is expressed in a large variety of non-cholinergic, non-cholinceptive tissues and generates at least three different proteins with distinct C termini produced by alternative splicing. These likely differ in their non-catalytic activities, independent of the acetylcholine-hydrolyzing capacity of AChE (21). An additional level of diversity is enabled by the different alternative first exons, suggesting a combinatorial complexity.

The alternative first AChE exons display expression profiles distinct from those of the 3' exons. This rules out the possibility that a particular first exon is strictly associated with a given 3' exon. The 3' splicing options of the murine and human AChEs (AChE-S, AChE-R, and AChE-E) may thus yield up to 15 and 12 different mRNA transcripts, respectively (Fig. 7). Diversified regulation at the 5'-untranslated region level may reflect yet unexplained roles for the 5' variants. For example, in the human fetus, hE1d mRNA was expressed in the nervous system and thymus in a developmentally regulated manner. In the fetal brain, hE1d mRNA was expressed in migrating neurons in both cell bodies and neuritic processes, and the number of hE1d-positive neurons grew from roughly undetected levels at week 16 to about 50% of the neurons at week 34, coinciding with the formation of synapses in these neurons. Further studies will be required to find whether this coincidence reflects a functional relationship.

N-terminally Extended N-AChE(s)—Of particular interest are the novel N-AChE protein(s) containing N-terminal extensions. The extended translation products displayed 79% sequence similarity in human and mouse with similarly high pI values and similar phosphorylation and *N*-myristoylation sites of the putative translation products, supporting the notion of physiological relevance. The classical human AChE protein includes a 31-amino acid residue signal peptide at its N terminus that is cleaved off during protein maturation. However, we predicted that adding hE1d to the AChE mRNA transcript and its translation product to the AChE protein would prevent the cleavage of this signal peptide. Under these conditions, the corresponding region in the AChE translation product would become a transmembrane domain in an N-terminally extended (and 16% larger) AChE variant (hN-AChE). Analogous situations have been described for the asialoglycoprotein receptor (20), adrenal dopamine β -monooxygenase (22), α -neurexin (an extended form of β -neurexin) (23), retinal RodX exchanger (24), prion protein (25), and cyclooxygenase (26). COX-1, the classic cyclooxygenase form, includes a signal peptide at the N terminus. A novel cyclooxygenase variant, COX-3, includes an unusually spliced nucleotidic sequence, which encodes for an N-terminal extension of the protein. This prevents the cleavage of the signal peptide, resulting in a transmembrane protein variant with distinct properties.

Membrane Properties of N-AChE—Antibodies generated against the hN-AChE peptide interacted with at least two brain-expressed polypeptides with electrophoretic properties similar to those of AChE, and several of the commercially available anti-AChE antibodies yield double bands around

⁴ See npsa-pbil.ibpc.fr/cgi-bin/secpred_gor4.pl.

⁵ See hits.isb-sib.ch/cgi-bin/PFSCAN.

⁶ See www.expasy.org/tools/tagident.html.

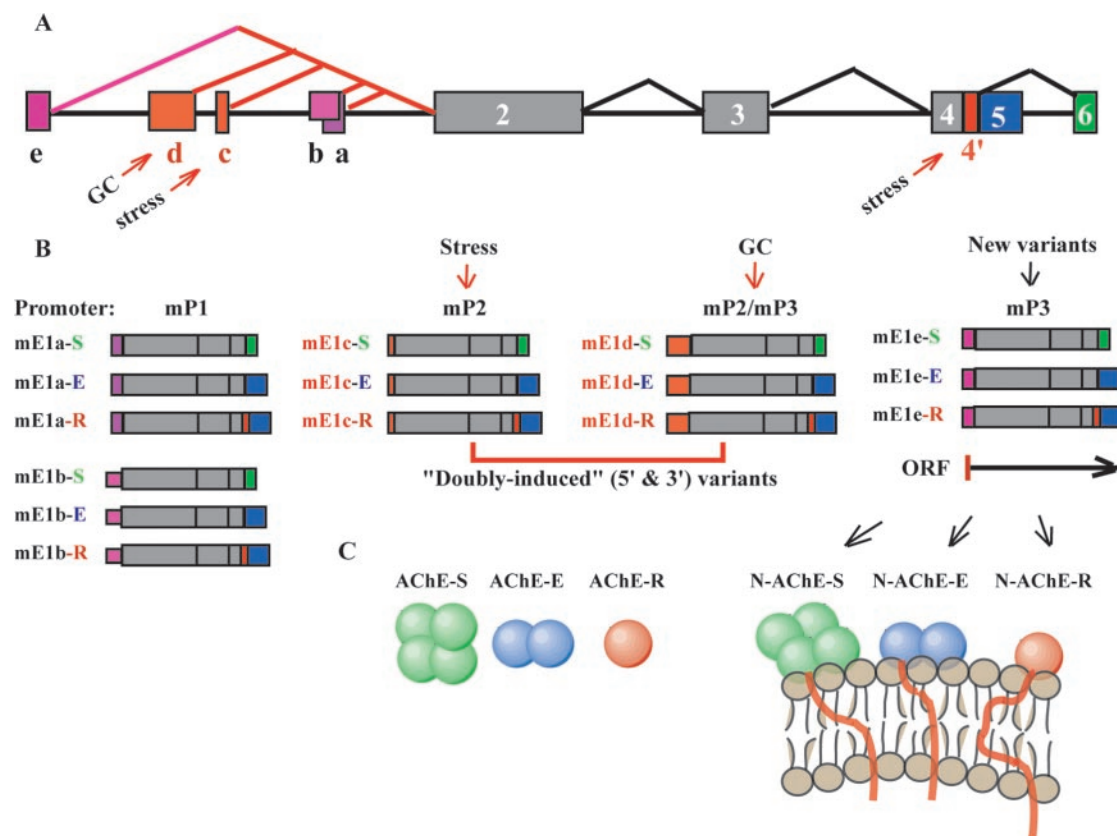


FIG. 7. **Predicted combinatorial complexity of the 5' and 3' AChE mRNA variants and their protein products.** Shown are the splice (A) and regulation patterns of the putative mouse *AChE* transcripts and their predicted promoters (B) and protein products (C). Arrows note enhancing stimuli (GC, glucocorticoids). Doubly induced variants (mE1c-R and mE1d-R) include both 5' and 3' exons that respond to glucocorticoids and stress. Extended N-AChE proteins may have one or more transmembrane domains at their N terminus.

66–70 kDa (for example, see Refs. 27–29). This supports the notion that at least part of the brain AChE proteins corresponds to N-terminal extended form(s). The N terminus of hN-AChE may enable monomeric AChE-S or AChE-R to traverse the membrane, conferring yet undefined physiological functions onto its cytoplasmic domain (Fig. 7). As a matter of fact, initial studies by Podleski and Changeux (30) suggested receptor-like function for membrane AChE (30). Direct docking of AChE to the synaptic membrane would explain its presence in brain regions lacking the proline-rich membrane anchor (PRiMA) subunit necessary to anchor AChE-S tetramers to the synapse (31, 32). This could have an especially significant outcome for poststress situations where large amounts of monomeric AChE are produced rapidly. Membrane targeting of the produced enzyme could be efficient for rapidly reducing the synaptic levels of acetylcholine, whereas its putative N-terminal phosphorylation and myristoylation can possibly transduce cytoplasmic signals.

Flow cytometry analyses demonstrated that, in blood cells, hN-AChE is primarily located in membranes. Monocytes, granulocytes, and lymphocytes were all positive albeit to different extents. In lymphocytes, hN-AChE levels increased from early to mature T-lymphocytes, possibly explaining the distinct expression patterns throughout thymic development. Indeed hE1d mRNA was expressed in RNA extracted from human leukemic T-cells but not from human embryonic stem cells. hN-AChE expression in T- and B-lymphocytes is compatible with reports of cholinergic regulation of lymphocyte function (33). Moreover exposure to anti-AChEs, which induce AChE overexpression (21), also involves an increased risk of leukemia (40). Our current findings point at N-AChE as a putative candidate in that process.

Electrostatic as well as covalent interactions of hN-AChE monomers having diverse C termini (e.g. AChE-E and AChE-S) can potentially create hN-AChE-associated multimers with complex structures. Unusual AChE forms have been reported in Alzheimer's disease (34, 35) and in dementia (36). Sucrose gradient analyses also reveal high diversity of the various AChE isoforms (37). Much of these observations could reflect these new, longer members of the AChE family, and the potent labeling of brain AChE-like proteins with anti-hN-AChE antibodies suggests multiregional abundance of such variants.

Density of Repeats—Alu repeats are the most abundant SINEs within the primate genome (14). In humans, 1.5 million SINEs account for some 13% of the genome, and the 850,000 LINEs account for another 21%, comprising together a grand total of 34% of the genome (38). LINEs are usually found in gene-poor, AT-rich areas; SINEs are preferentially located within gene-rich regions. During evolution, LINEs and SINEs replicate and/or move about the genome. Residing at or near transcriptionally active regions increases the rate of such events, while interference with transcription can be deleterious (14). These opposing forces lead to the accumulation of repeats near to, but not inside, transcriptionally active sites. The human and mouse *AChE* genes demonstrated an inverse association between the repeat density in transcribed units as compared with 5' upstream sequences, compatible with parallel findings in most functional transcription units (14). Since *AChE* is a ubiquitously active gene, such accumulation of repeats is not surprising. The absence of repeats from the 3.5-kb exon-containing region, in view of the dense repeat population in this locus, further supports the notion that the novel first exons are functionally active and carry out evolutionarily advantageous roles.

Differential Expression Patterns—Alternative first exons could influence the cellular and subcellular distribution of the different transcripts. In brain neurons, AChE mRNA is subject to stress-related regulation and neuritic translocation (6). Stress-responding neurons display replacement of dendritic AChE-S with AChE-R mRNA, and it remains to be tested which of the newly identified first exons are similarly regulated. None of the three 5' murine probes tested (mE1a, mE1b, and mE1d) showed dendritic expression in control mice, but in murine Purkinje cells, mE1d presented an unusual subcellular expression in both cell bodies and axons. Axonally deposited mRNA transcripts are known albeit rare (39). This observation poses novel questions regarding the expression pattern and the physiological function of AChE in Purkinje cells in general and in axonal processes in particular.

Expression in Response to Stress—We wished to find out whether the newly described transcripts are differentially regulated under stress and, if so, whether the stress-induced release of GCs is involved. Various putative DNA binding elements that could be involved in induction of *ACHE* expression, including GRE, AP1, and cAMP-response element-binding protein, are present in the different promoter regions. One GRE site was identified within mE1d, and two were identified upstream to mE1b. AP1 sites were found in mP2 and mP3. We therefore studied the expression of the different AChE mRNA variants in response to immobilization stress both in control (GR^{LoxP/LoxP}) and in mice deprived of GR in neurons and glial cells (GR^{NesCre} mice (9)). Two different variants, mE1c and mE1d, were found to be induced in response to stress. Of these two, mE1d but not mE1c requires the activation of GR for its induction. In contrast, both mE1b and AChE-S were repressed under stress but only in GR^{NesCre} mice. One possible explanation could be that following stress, contrasting effects of different factors, among them glucocorticoids, cancel out one another, keeping the levels of mE1b unaltered. In the absence of GRs, the GREs are no longer functional, and maintained activities of suppressing factors may then reduce mE1b levels.

In conclusion, the existence of novel 5' alternative splicing patterns of AChE mRNA has important consequences. First and foremost, they extend the complexity and versatility of AChE mRNA variants to levels that were not previously perceived. In addition, the 5' splice variations yield N-terminally extended membrane variant(s) of AChE in brain neurons and hematopoietic cells. While the C-terminal composition and membrane directionality of these variants await further research, this finding explains certain long known enigmas in AChE research and opens numerous new questions. The apparent conservation of this extended domain in rodents and primates strengthens its biological relevance. Its unique expression patterns and stress-associated regulation call for exploring its physiological significance.

Acknowledgments—We thank Alastair Grant (London, UK) for early contributions to this work, Shoshana Baron and Marjorie Pick (Tel-Aviv, Israel) for technical assistance, Drs. Micha Drukker and Nissim

Benvenisty (Jerusalem, Israel) for human embryonic stem cells, and Dr. David Glick (Jerusalem, Israel) for critically reviewing this manuscript.

REFERENCES

- Graveley, B. R. (2001) *Trends Genet.* **17**, 100–107
- Cramer, P., Pesce, C. G., Baralle, F. E., and Kornblihtt, A. R. (1997) *Proc. Natl. Acad. Sci. U. S. A.* **94**, 11456–11460
- Modrek, B., Resch, A., Grasso, C., and Lee, C. (2001) *Nucleic Acids Res.* **29**, 2850–2859
- Xie, H., Zhu, W. Y., Wasserman, A., Grebinskiy, V., Olson, A., and Mintz, L. (2002) *Genomics* **80**, 326–330
- Sorek, R., and Safer, H. M. (2003) *Nucleic Acids Res.* **31**, 1067–1074
- Meshorer, E., Erb, C., Gazit, R., Pavlovsky, L., Kaufman, D., Friedman, A., Glick, D., Ben-Arie, N., and Sorek, H. (2002) *Science* **295**, 508–512
- Mutero, A., Camp, S., and Taylor, P. (1995) *J. Biol. Chem.* **270**, 1866–1872
- Atanasova, E., Chiappa, S., Wieben, E., and Brimjoin, S. (1999) *J. Biol. Chem.* **274**, 21078–21084
- Tronche, F., Kellendonk, C., Kretz, O., Gass, P., Anlag, K., Orban, P. C., Bock, R., Klein, R., and Schutz, G. (1999) *Nat. Genet.* **23**, 99–103
- Li, Y., Camp, S., Rachinsky, T. L., Getman, D., and Taylor, P. (1991) *J. Biol. Chem.* **266**, 23083–23090
- Ben Aziz-Aloya, R., Sternfeld, M., and Sorek, H. (1993) *Prog. Brain Res.* **98**, 147–153
- Sorek, H., Ben-Aziz, R., Prody, C. A., Seidman, S., Gnat, A., Neville, L., Lieman-Hurwitz, J., Lev-Lehman, E., Ginzberg, D., Lipidot-Lifson, Y., and Zakut, H. (1990) *Proc. Natl. Acad. Sci. U. S. A.* **87**, 9688–9692
- Panganiban, G., and Rubenstein, J. L. (2002) *Development* **129**, 4371–4386
- Batzer, M. A., and Deininger, P. L. (2002) *Nat. Rev. Genet.* **3**, 370–379
- Wilson, M. D., Riemer, C., Martindale, D. W., Schnupf, P., Boright, A. P., Cheung, T. L., Hardy, D. M., Schwartz, S., Scherer, S. W., Tsui, L. C., Miller, W., and Koop, B. F. (2001) *Nucleic Acids Res.* **29**, 1352–1365
- Drukker, M., Katz, G., Urbach, A., Schuldiner, M., Markel, G., Itskovitz-Eldor, J., Reubinoff, B., Mandelboim, O., and Benvenisty, N. (2002) *Proc. Natl. Acad. Sci. U. S. A.* **99**, 9864–9869
- Kaufman, D., Friedman, A., Seidman, S., and Sorek, H. (1998) *Nature* **393**, 373–377
- Shapira, M., Tur-Kaspa, I., Bosgraaf, L., Livni, N., Grant, A. D., Grisaru, D., Korner, M., Ebsstein, R. P., and Sorek, H. (2000) *Hum. Mol. Genet.* **9**, 1273–1281
- Rachinsky, T. L., Camp, S., Li, Y., Ekstrom, T. J., Newton, M., and Taylor, P. (1990) *Neuron* **5**, 317–327
- Spies, M., and Lodish, H. F. (1986) *Cell* **44**, 177–185
- Sorek, H., and Seidman, S. (2001) *Nat. Rev. Neurosci.* **2**, 294–302
- Taljanidisz, J., Stewart, L., Smith, A. J., and Klinman, J. P. (1989) *Biochemistry* **28**, 10054–10061
- Ushkaryov, Y. A., Hata, Y., Ichtchenko, K., Moomaw, C., Afendis, S., Slaughter, C. A., and Sudhof, T. C. (1994) *J. Biol. Chem.* **269**, 11987–11992
- McKiernan, C. J., and Friedlander, M. (1999) *J. Biol. Chem.* **274**, 38177–38182
- Stewart, R. S., Drisaldi, B., and Harris, D. A. (2001) *Mol. Biol. Cell* **12**, 881–889
- Chandrasekharan, N. V., Dai, H., Roos, K. L., Evanson, N. K., Tomsik, J., Elton, T. S., and Simmons, D. L. (2002) *Proc. Natl. Acad. Sci. U. S. A.* **99**, 13926–13931
- Brenner, T., Hamra-Amitay, Y., Evron, T., Boneva, N., Seidman, S., and Sorek, H. (2003) *FASEB J.* **17**, 214–222
- Morel, N., Leroy, J., Ayon, A., Massoulie, J., and Bon, S. (2001) *J. Biol. Chem.* **276**, 37379–37389
- Belbeoch, S., Massoulie, J., and Bon, S. (2003) *EMBO J.* **22**, 3536–3545
- Podleski, T., and Changeux, J. P. (1967) *Science* **157**, 1579–1581
- Perrier, A. L., Massoulie, J., and Krejci, E. (2002) *Neuron* **33**, 275–285
- Perrier, N. A., Kherif, S., Perrier, A. L., Dumas, S., Mallet, J., and Massoulie, J. (2003) *Eur. J. Neurosci.* **18**, 1837–1847
- Kawashima, K., and Fujii, T. (2000) *Pharmacol. Ther.* **86**, 29–48
- Navaratnam, D. S., Priddle, J. D., McDonald, B., Esiri, M. M., Robinson, J. R., and Smith, A. D. (1991) *Lancet* **337**, 447–450
- Darreh-Shori, T., Hellström-Lindahl, E., Flores-Flores, C., Guan, Z., Sorek, H., and Nordberg, A. (2004) *J. Neurochem.* **88**, 1102–1113
- Shen, Z. X. (1997) *Neuroreport* **8**, 3229–3232
- Massoulie, J. (2002) *Neurosignals* **11**, 130–143
- Weiner, A. M. (2002) *Curr. Opin. Cell Biol.* **14**, 343–350
- Job, C., and Eberwine, J. (2001) *Nat. Rev. Neurosci.* **2**, 889–898
- Pick, M., Flores-Flores, C., Grisaru, D., Shochat, S., Deutsch, V., and Sorek, H. (2004) *Int. J. Dev. Neurosci.*, in press